

# Synthesis of Vixotrigine, a Voltage- and Use-Dependent Sodium Channel Blocker. Part 2: Development of a Late-Stage Process

Robbie Chen, Vincent Couming, John Guzowski, Jr., Erwin Irdam, William F. Kiesman, Daw-Long Albert Kwok, Wenli Liang, Tamera Mack, Erin M. O'Brien, Suzanne M. Opalka, Daniel Patience, Stefan Sahli, Donald G. Walker,\* Frederick Osei-Yeboah, Chaozhan Gu, Xin Zhang, Markus Stöckli, Thiemo Stucki, Hanspeter Matzinger, Roman Kuhn, Michael Thut, Markus Grohmann, Benjamin Haefner, Joerg Lotz, Michael Nonnenmacher, and Paolangelo Cerea



Cite This: <https://dx.doi.org/10.1021/acs.oprd.0c00427>



Read Online

ACCESS |

Metrics & More

Article Recommendations

**ABSTRACT:** As vixotrigine (**1**) entered a later clinical phase for trigeminal neuralgia (Zakrzewska, J. M.; et al. *Lancet Neurol.* **2017**, *16*, 291–300), the development of a sustainable late-stage process was required to meet the supply needs for formulation optimization, phase 3 clinical trials, and registration stability batches (this is the expected commercial formulation). In this article, we describe how the process was streamlined from the early supply route (Giblin, G.; et al. *Org. Process Res. Dev.* **2020**, DOI: [10.1021/acs.oprd.0c00382](https://doi.org/10.1021/acs.oprd.0c00382)) and a comprehensive control strategy was established. Process improvements included improving safety and scalability for a temperature-sensitive Grignard reaction, simplifying unit operations, removal of heterogenous conditions, and route redesign to afford a high yielding, one-pot sequential alkylation and amidation. Improvement in the salt formation step, combined with wet milling, resulted in improved particle properties with enhanced flow properties of the final active pharmaceutical ingredient. The process mass intensity was improved 65% while maintaining drug substance purity at more than 99.8%. This new process has been scaled up to generate metric ton quantities of drug substance.

**KEYWORDS:** *flow chemistry, telescoped reactions, wet milling, manufacturing process*

## INTRODUCTION

Chronic pain can make life challenging for sufferers and leave patients with significantly disrupted lives.<sup>1</sup> Vixotrigine (**1**) (Figure 1) is a nonopioid, voltage- and use-dependent sodium

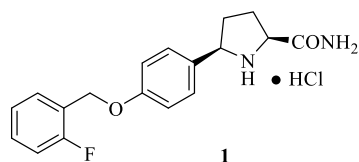


Figure 1. Structure of vixotrigine.

channel blocker currently being studied for the management of neuropathic pain conditions and has shown efficacy in a phase 2 clinical study for pain associated with trigeminal neuralgia.<sup>2</sup> Two manufacturing processes for vixotrigine were described in the preceding article, an enabling kilo lab route adapted from the medicinal chemistry synthesis and an improved pilot scale process for early and midphase clinical supplies. To support phase 3 studies and late-stage manufacturing, a more robust process was required that would enable delivery of metric ton quantities of **1**. Here, we describe our studies leading to the current manufacturing process for the synthesis of vixotrigine.

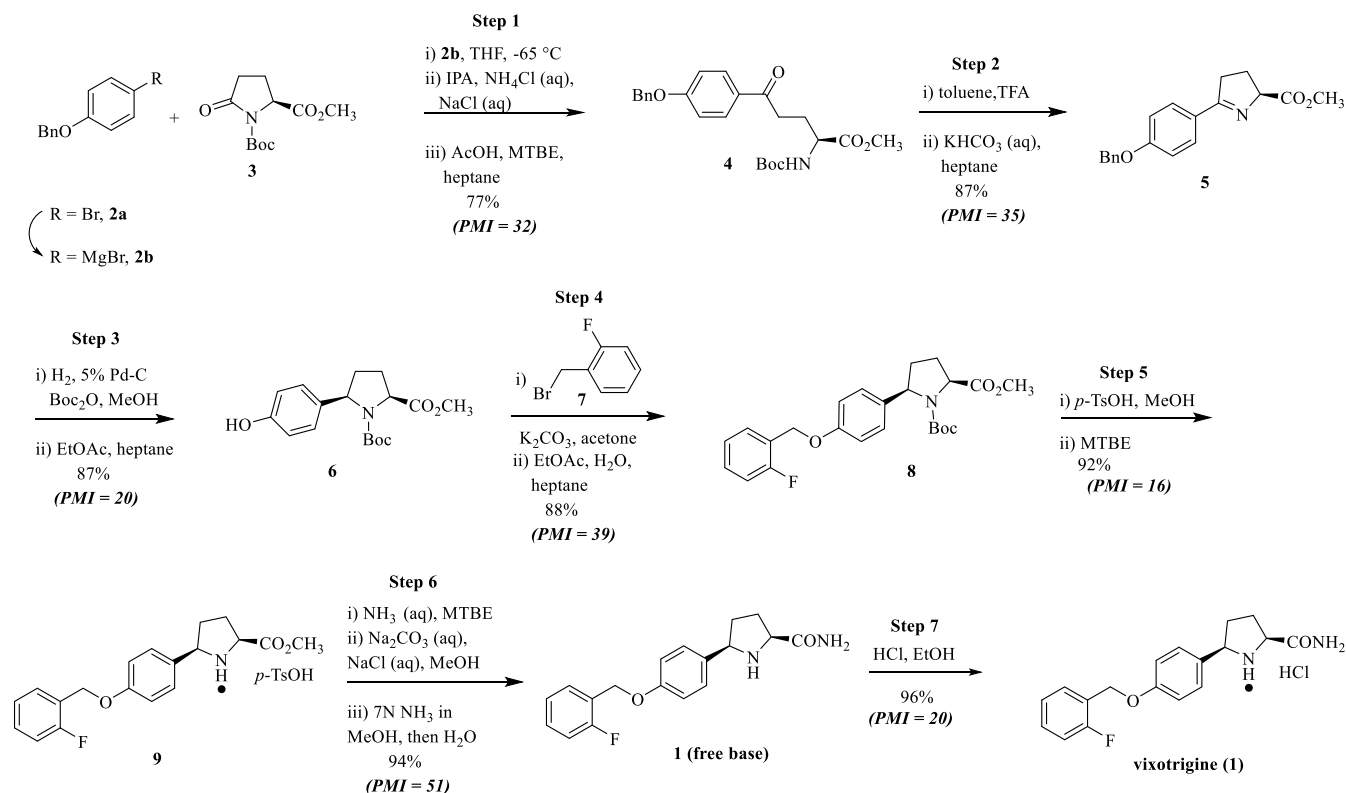
## PROCESS DEVELOPMENT STRATEGY

Of the two routes previously developed and implemented for the manufacture of vixotrigine, the pilot scale process (Scheme 1) was developed for the early phase delivery of clinical trial materials,<sup>3</sup> however, further improvements were necessary to address larger-scale process considerations. These included a reduction in cost of goods, a decrease in process mass intensity (PMI),<sup>4</sup> shorter cycle times, and scale increases because of a projected high-volume demand for vixotrigine. The first step of the synthesis was considered challenging for the high volume needs of late-stage manufacturing given the capacity constraints for large-scale cryogenic (−70 °C) reactions. Engineering solutions were examined to address these challenges in batch reactors and a flow process was also developed (step 1). An additional critical optimization included increasing the selectivity and throughput of a selective one-pot catalytic imine reduction and benzyl group hydrogenolysis, with a concomitant Boc protection of the pyrrolidine formed, to afford intermediate **6**. Optimization of step 6 was deemed necessary

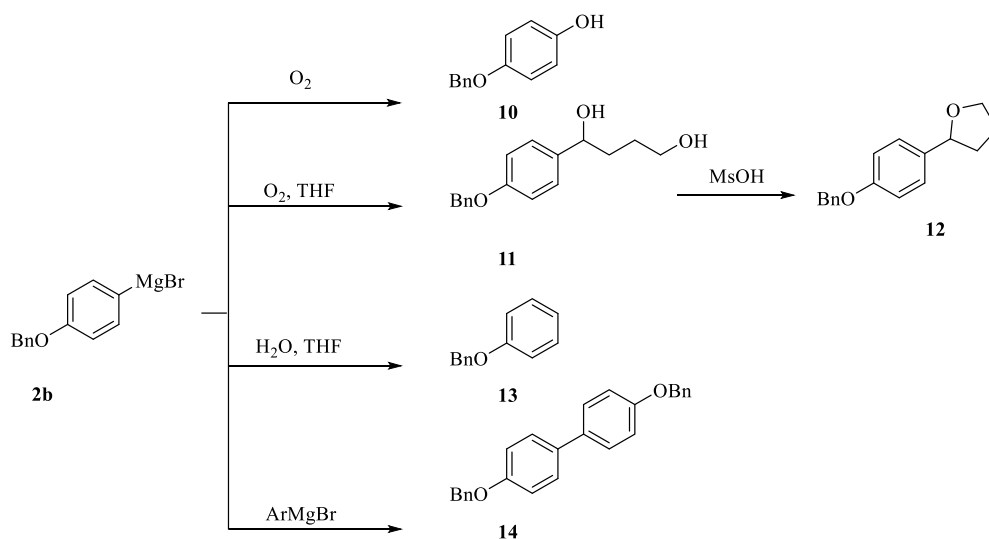
Received: September 25, 2020



Scheme 1. Pilot Scale Process for Vixotrigine (1)



Scheme 2. Observed Process Impurities in the Grignard Formation



because of the difficulty of removing *p*-TsOH and the time-consuming amidation reaction using methanolic ammonia. An opportunity was seen to reorder the alkylation–deprotection–amidation sequence, bringing two basic steps in tandem to allow for a one-pot process saving solvent and processing time. The HCl salt formation from the early supply route resulted in a drug substance with a small particle size distribution (PSD) unsuitable for the formulation process. Alternative salt-forming conditions and wet-milling technology were chosen to engineer the particles to meet the desired flow properties.

## RESULTS AND DISCUSSION

The Grignard reagent formation and reaction with pyroglutamate **3** to generate **4** had several scale-dependent challenges, including volume inefficiency (PMI = 32), moderate yields, and requirement of cryogenic reaction temperatures. The clinical timeline did not allow enough time to develop, demonstrate, and scale a novel flow process to address these challenges, so the batch process was optimized to supply materials quickly, and, in parallel the development of a flow process to completely remove the cryogenic temperature requirements was undertaken.

**Grignard Reaction: Batch Processing.** The pilot scale process needed improvement in a few key areas for successful

scale up. First, the process utilized a high-temperature dry activation protocol involving heating iodine and magnesium turnings at 105 °C for 3 h to prepare Grignard reagent **2b** at a 17 kg scale. This procedure could lead to inhomogeneous activation and was not preferred for scale up. In addition, the reaction quench was complex, and the workup required a lengthy solvent concentration of the methyl *tert*-butyl ether (MTBE) mixture after extraction prior to precipitation with hexane. The Grignard addition reaction between **2b** and **3** was performed in tetrahydrofuran (THF) at -65 °C using 1.75 equiv of 1-(benzyloxy)-4-bromobenzene (**2a**) and after quenching and workup, the product was isolated from MTBE/heptane to provide **4** in 78% yield, with 98.7% w/w purity. The major process impurity in this initial run was the Wurtz<sup>5</sup> homo-coupled impurity **14** (Scheme 2), observed at 0.68% w/w.

The focus of process optimization was to ensure safety, streamline reagent choice with attention to stoichiometry, and reduce reaction and workup volumes to maximize the reaction throughput. The dry magnesium metal and iodine initiation protocol was replaced with one using 1 M DIBAL-H in toluene.<sup>6</sup> The safety of the initiation was improved, and the use of 1,2-dibromoethane was eliminated. Furthermore, the improved process reduced the amount of magnesium to 1.05 equiv relative to **2b** thereby reducing the quenching solvent volumes during cleaning. Summarized below in Table 1 is a comparison of the pilot scale and improved magnesium activation protocols.

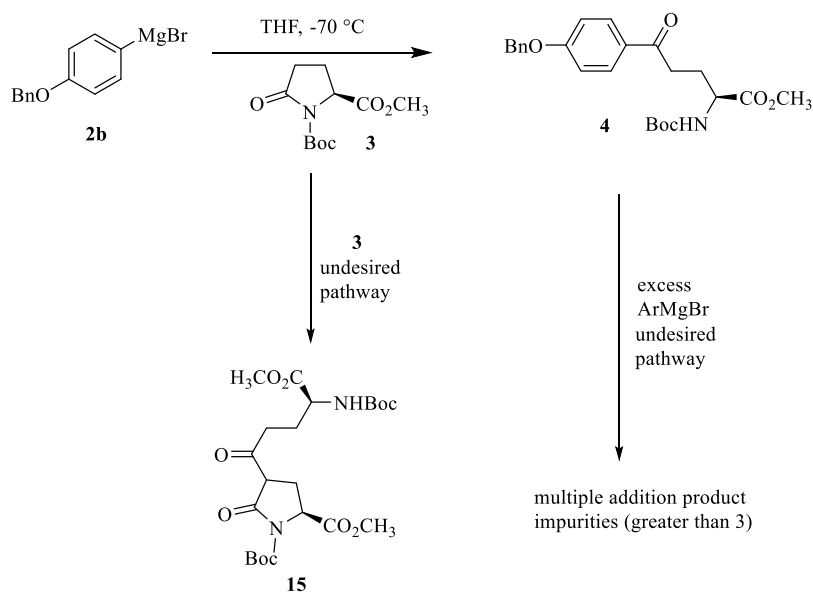
**Table 1. Comparison of Magnesium Activation Protocols**

Pilot Scale	process improvements	New Process
i) I <sub>2</sub> , Mg, 105 °C, N <sub>2</sub>		i) Mg, THF, DIBAL-H / PhMe; reflux
ii) cool to 30 °C		ii) add 5% of <b>2a</b> solution
iii) add I <sub>2</sub> , THF; reflux		iii) hold and confirm initiation
iv) add <b>2a</b> solution over 6 h		
v) add 1,2-dibromoethane (30 min after step iv start)		

During process exploration, Grignard-related impurities from reactions with oxygen [**10**, **11**, and **12** (produced from **11** in step 2)] or moisture (**13**) and homo-coupling (**14**) were observed (Scheme 2).<sup>7</sup> The assay value for the Grignard reagent **2b** was stable when under a nitrogen atmosphere. However, upon ceasing the nitrogen feed and exposing the solution to air, an immediate and sustained increase in phenol impurity **10**, THF adduct impurity **11**, and des-bromo impurity **13** was observed (Scheme 2). Therefore, stringent atmospheric controls were developed to avoid the introduction of oxygen in both the Grignard formation phase as well as the cooling phase prior to the addition of **3**. To ensure air-free conditions, THF was heated under reflux in a nitrogen atmosphere for degassing prior to charging to the reactor. Check valves were also installed on vent lines to further minimize air exposure. Reaction of **3** with itself to form **15**, and multiple addition products as shown in Scheme 3 were another source of yield loss. To address this issue, low-temperature conditions were used and reduced equivalents of the Grignard reagent **2b** were implemented.

The earlier direct quench of the Grignard addition reaction with 2-PrOH at -60 °C was replaced by a simplified reverse quench whereby THF/2-PrOH was prepared in a separate reactor and the -60 °C reaction mixture was added keeping the quench solution above -20 °C. This simple change used the lower temperature of the Grignard reaction solution to control temperature during the quench. Addition of water followed by adjustment to pH 6–7 with 50% aqueous acetic acid followed by a final wash of the organic phase with brine completed the workup. After a filtration to remove the magnesium particles, the solution was taken directly for crystallization from THF/heptane. The elimination of the lengthy MTBE solvent swap in favor of a simple crystallization from the partially concentrated organic reaction solution and the direct processing of wet **4** forward into the next step streamlined the process further. Although the average yield of the optimized Grignard reaction sequence remained similar (74%), Wurtz impurity **14** was not detected in **4** and the volume efficiency almost doubled (PMI from 32 to 17).

**Scheme 3. Proposed Impurities in Step 1 Impacting the Mass Balance**



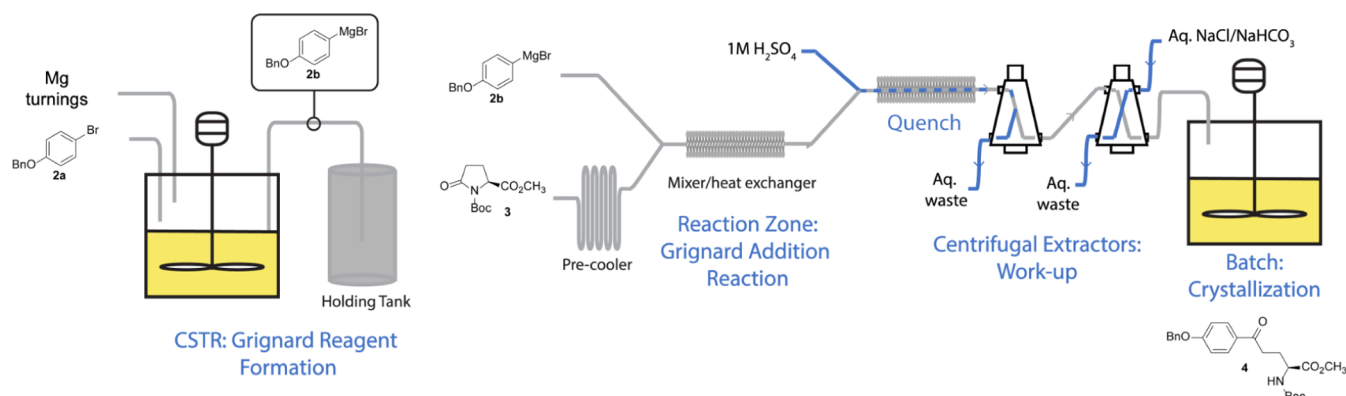


Figure 2. Overview of the flow process flow design for Grignard addition and workup.<sup>11</sup>

**Grignard Reaction: Flow Processing.** Utilization of suitable flow process equipment enables precise temperature control by fast mixing and effective heat exchange.<sup>8</sup> These benefits often result in improved quality of the isolated product and more robust manufacturing processes.<sup>9,10</sup> Given the projected high volume demand for vixotrigine, it was important to avoid the large-scale Grignard initiations and limit the need for cryogenic reactor capacity required for batch operation.

Various equipment configurations were considered for all unit operations in the preparation of **4** (Grignard reagent formation, Grignard addition, quench, and phase separation) except the final crystallization, which adapted the THF/heptane protocol from the batch process to isolate the product. A flow setup was designed (Figure 2) utilizing:

- a continuous stirred tank reactor (CSTR) for Grignard formation
- a plug flow reactor for Grignard addition and quench
- centrifugal extractors for phase separations and washes

CSTR strategies<sup>12</sup> for the formation of Grignard reagents have been published previously. For this project, a setup was established to specifically suit the conversion of **2a** to **2b**. The main challenges are related to charging magnesium and reaction monitoring. The key challenge for the addition of Grignard reagent **2b** to **3** in flow was implementing a reactor design that avoided clogging and incorporated the quench. The final equipment train featured a two tank CSTR setup for Grignard formation. In the first tank, the Grignard formation occurred. For this, a 500 mL vessel was fitted with:

- a solid addition device for magnesium addition
- an inlet for delivery of **2a**
- a sampling port
- a product removal tube for transfer of the contents to a second tank to settle solids before further transfer

Capitalizing on learnings from the batch process, the entire reaction was kept under an inert atmosphere (Scheme 2). The advantage of a CSTR setup was that fresh **2a** and magnesium could be charged continuously to an already activated tank of the Grignard reagent, obviating the need for initiation with each charge of fresh reactants. Initiation was confirmed by measurement of an exotherm and observation of a change in color. Once observed, the starting feeds of bromide **2a** in THF and magnesium were added at such a rate that allowed for a 60 min residence time for Grignard formation. The setup was designed in a way to allow transfer of the product solution via a settling tank to storage without displacement of magnesium particles. This feed solution of **2b** in THF was prepared at a

concentration of 0.83 M and the setup was run for 18 h to provide 10 kg of the Grignard solution to process forward in the addition step.

For reaction of **2b** with pyroglutamate **3**, the flow setup consisted of a plug flow reactor to allow efficient mixing of two feed streams and a mixer/heat exchanger. Three reagent streams (**2b**, **3**, and quench solution) were charged from stainless steel vessels and regulated by mass flow metering valves to achieve the desired stoichiometry (1.25 equiv **2b**/1.0 equiv **3** for the reaction and 1.0 equiv 1 M sulfuric acid for the quench). The pyroglutamate **3** solution was pre-cooled by passing through a heat exchanger to reach a temperature of  $-8\text{ }^{\circ}\text{C}$ . The pyroglutamate **3** and **2b** were mixed and passed directly into a mixer/heat exchanger that efficiently removed heat generated during the reaction. The entire residence time was under 8 s before quenching with 1 M sulfuric acid.

The concentration and temperature of the quench were chosen to completely dissolve the magnesium sulfate instantaneously upon mixing. After the sulfuric acid quench, phase separation was achieved with centrifugal extractors followed by a brine wash. Direct collection of the THF product stream into a reactor and crystallization of **4** after the addition of heptane antisolvent gave a wet cake of intermediate **4** that after drying produced a total of 1.77 kg (84%) based on **3**. Summarized below in Table 2 is a comparison of the improved batch and flow process results for producing ketone **4**.

The PMI for the flow process was comparable to the batch process; however, flow processing avoids cryogenic conditions and affords flexibility in scaling. Work is currently ongoing to scale up the flow process using manufacturing equipment.

Table 2. Comparison of the Improved Batch and Flow Process Results for Producing **4**

parameter	improved batch	flow
scale (kg <b>3</b> )	284.9	1.20
reaction temperature	$<-50\text{ }^{\circ}\text{C}^a$	$\sim 10\text{ }^{\circ}\text{C}^b$
isolated <b>4</b> (kg)	375 <sup>c</sup>	1.77
% yield	74 <sup>c</sup>	84
PMI	17	15
purity	97.0 <sup>d</sup>	98.6 <sup>e</sup>
residual <b>14</b> (Wurtz)	ND <sup>f</sup>	ND <sup>f</sup>

<sup>a</sup>Internal reaction temperature maintained during the addition of **2b** to **3**. <sup>b</sup>Reaction temperature measured before the quench. <sup>c</sup>Based on wet cake loss on drying (LOD). <sup>d</sup>Wet cake assay (% w/w vs a characterized reference standard). <sup>e</sup>Assay (% w/w). <sup>f</sup>Not detected.

**Imine Formation.** Acid-promoted deprotection of **4** and subsequent cyclization gave imine **5** in a single step and although high yielding for pilot scale, areas for further development included enhanced impurity control, use of low cost alternative acids, and optimization of the workup volumes. Significant excesses of TFA (8.9 equiv) and the tedious neutralizing quench workup contributed to lengthy unit operations and generation of unnecessary waste. The major impurities observed in isolated imine **5** were the hydrolysis product **16** ( $\leq 0.50\%$ ) and enantiomer **17** ( $\leq 0.16\%$ ) (Figure 3).

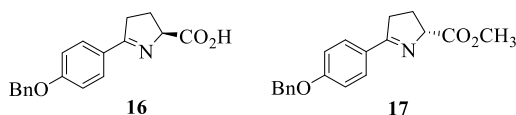


Figure 3. Major process impurities for the synthesis of **5**.

Solvent screening identified acetonitrile (ACN) as an optimal toluene replacement for imine formation, allowing for increased volume efficiency [3 V (L/kg starting material) vs 6.5 V respectively]. Additionally, any low level Wurtz impurity **14** carried over from the previous step was insoluble in ACN and could be removed easily by filtration. Methanesulfonic acid readily replaced TFA and the conversion to imine **5** was accomplished with only 2.9 equiv, which reduced the quench volume and cycle time.

Attention was then turned to focus on the parameters controlling levels of impurities **16** and **17**. Formation of the acid impurity **16** increased if the reaction temperature was  $>30\text{ }^{\circ}\text{C}$ , if the water content within the reaction was high, or if the apparent pH was held at  $<1$  during the quench procedure. Specifically, when the reaction was run at  $35\text{ }^{\circ}\text{C}$ , an increase of **16** to 3.4 area % was observed. The addition of adventitious water (1.0 equiv) to the reaction produced 2.1 area % of **16**. Optimization experiments on the workup found that when 25% of the quench solution (4.6 N  $\text{NH}_4\text{OH}$ ) was added (apparent pH  $<1$ ) and the reaction was held at  $15\text{ }^{\circ}\text{C}$  for 12 h, acid **16** was observed at 13.3 area %. However, when 40% of the quench solution was added (apparent pH 3) and the reaction was held at  $15\text{ }^{\circ}\text{C}$ , the level of **16** observed was only 0.26 area %.

A hold time study was conducted to determine the impact of pH and temperature on epimerization (Figure 4). Racemization

was least pronounced at pH 7.5 as both lower and higher pH values (6.5 and 8.5) resulted in more rapid rates of epimerization. Higher hold temperatures enhanced epimerization rates at all pH ranges, particularly at temperatures above  $25\text{ }^{\circ}\text{C}$ . It is likely that protonation of the imine nitrogen in **5** enhances the acidity of the ester  $\alpha$ -proton on the stereogenic center, promoting increased epimerization to **17**. With the results of these experiments in hand, the wet cake of **4** was first washed with ACN, and the reaction temperature was kept at  $<26\text{ }^{\circ}\text{C}$  to suppress the formation of acid **16**. A two-stage addition of quench solution was used, first with a rapid addition to achieve pH 3 (to ensure control of acid **16**) followed by a slower charge to the target pH of 7.5 (to avoid epimerization to enantiomer **17**). Finally, a water wash of the wet cake was added to ensure purging of acid **16** to the mother liquor.

Replacement of aqueous potassium bicarbonate with ammonium hydroxide cuts workup volumes by 85% and eliminated off-gassing. A cooling crystallization of **5** was performed in ACN/2-PrOH (5:1 v/v) using water as the antisolvent (2 V), with seeding. The implemented process changes afforded 475 kg batches of crystalline **5** in  $>85\%$  yield,  $>99.5\%$  purity, and  $>99.5\%$  stereochemical purity [high-performance liquid chromatography (HPLC) area %]. The step 2 PMI was lowered from 35 to 20.

**Synchronized Imine Reduction, Amine Protection, and Debonylation.** The conversion of imine **5** to phenol **6** in the early pilot route involved three sequential chemical reactions, as shown in Scheme 4: reduction of imine **5** to give pyrrolidine **18**, followed by in situ Boc protection of the pyrrolidine nitrogen to produce **19** and then a reductive cleavage of the benzyl ether to afford phenol **6**.

Impurities observed during process optimization and scale up, listed in their order of decreasing importance, are shown in Figure 5 and include the pyrrolidine ring-opened impurity **20**, the impurity **21** arising from the reaction of the phenolic OH group in **6** with Boc-anhydride and the *trans*-epimer **22**. Other impurities of concern included the phenol **23**, arising from reductive cleavage of the benzyl group in **18** prior to the formation of the *N*-Boc intermediate **19**, the amino ester **24**, from ring-opening reduction of the C–N benzylic bond in **23**, and the phenol **25**, from reductive cleavage of the benzyl group in the imine **5** prior to the reduction of the imine function itself. When the hydrogenation was performed in the absence of

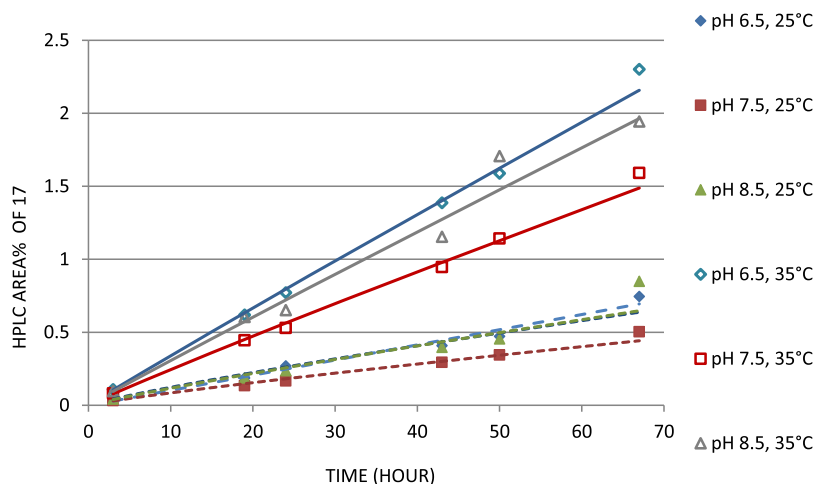


Figure 4. Growth of epimerization product **17** as a function of pH and temperature.

## Scheme 4. Transformations in the Conversion of 5 to 6 in Step 3

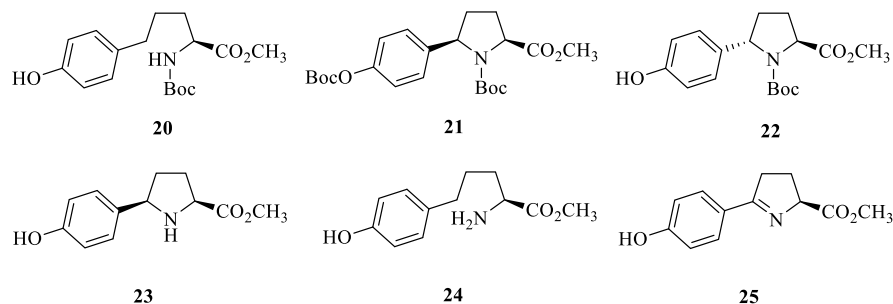
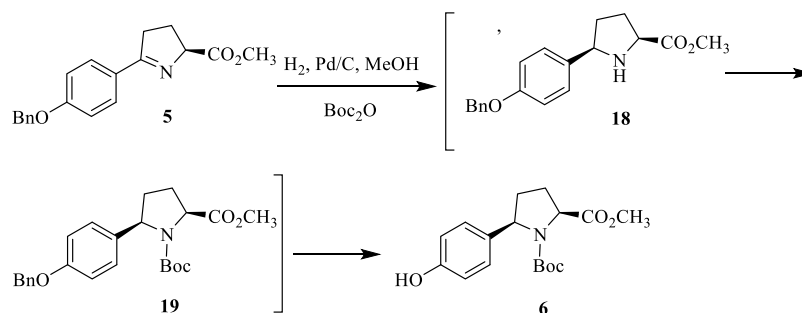


Figure 5. Impurities formed in step 3.

Table 3. Selected Catalyst Screening Results (2 h)<sup>a</sup>

entry	catalyst	JM catalog no.	5 (starting material)	22 (trans)	20 (ring-opened)	19 (OBn ether)	6 (product)
1	5% Pd/C type 487 (7.5 wt %)	113045	ND <sup>b</sup>	0.17	0.56	68.9	30.3
2	20% Pd(OH) <sub>2</sub> /C (1 wt %)	A401002-20	ND	0.19	0.31	78.0	21.7
3	5% Pt/C (1 wt %)	B103032-5	6.3	ND	ND	93.6	0.09
4	5% Pd/C (1 wt %)	5R58	85.3	ND	ND	14.5	0.18

<sup>a</sup>Area % purity by HPLC. <sup>b</sup>Not detected.

Boc<sub>2</sub>O, impurities **23** (65 area %) and **24** (34 area %) are the major observed species; when the anhydride was not present in excess, these impurities were observed at higher levels.

After initial evaluation of the pilot scale conditions, the following parameters were targeted for additional studies: reducing the Boc<sub>2</sub>O charge, lowering the catalyst charge below 7.5 wt % or, changing the catalyst, decreasing the reaction time and eliminating multiple distillations in the solvent swap from MeOH to EtOAc/heptane for product isolation.

Small-scale catalyst-screening experiments were performed with a variety of commercially available Pd/C and Pt/C catalysts from Johnson Matthey<sup>13</sup> to find a more active catalyst than 5% Pd/C type 487 paste and to address both the quantity of the catalyst charge and the long reaction time required for step 3 (Table 3).

Pt-based catalysts did not debenzylate well and produced **19** as the major reaction product and, therefore, these catalysts were not pursued further. Of the Pd/C catalysts screened, the use of Pearlman's catalyst [20 wt % Pd(OH)<sub>2</sub>/C] at a loading of 1 wt % (entry 2) gave encouraging results as compared with the use of 5% Pd/C type 487 at a loading of 7.5 wt % (entry 1). Further optimization studies indicated that the use of 3 wt % Pearlman's catalyst resulted in consistent completion of the reaction within 2–5 h. Pearlman's catalyst appeared to produce a more active Pd(0) catalytic species *in situ* in comparison to the use of the 5% Pd/C type 487 catalyst.<sup>14</sup> In addition, Pearlman's catalyst increased the rate of the reduction reaction in step 3 and was not susceptible to catalyst deactivation in alcoholic solutions.<sup>15</sup> After

that, catalyst selection attention was turned to optimizing the charge of Boc-anhydride. Ultimately, 1.01 equiv of Boc-anhydride afforded the best impurity profile for reactions that went to completion ( $\leq 0.15$  area % **19** with respect to **6**). The effect of added acetic acid on the impurity profile was briefly studied with the tepid results. For example, in one reaction employing 0.6 equiv, a reduced amount of **20** was observed (2.6 vs 3.6 area %); however, at the expense of more **23** (2.0 vs 0.68 area %); levels of **22** in each reaction were similar (0.31 vs 0.39 area %). In general, temperature and the agitation rate had little impact on the conversion rate to product **6** and product impurity profiles at reaction completion (reactions on 50–75 g scale, at 25 °C, 750 rpm; 35 °C, 500 rpm; and 35 °C, 750 rpm all afforded **6** in >93 area %).<sup>16</sup>

The pilot procedure for isolation of **6** required three distillations to solvent swap from MeOH to EtOAc, after which a charge of *n*-heptane induced crystallization. Crystallization of phenol **6** directly from MeOH was investigated and gave purified **6** in 90–92% yield from 1:1 (v/v) MeOH/water (4 V). In all experiments, phenol impurities **20** and **22** and Boc-phenol impurity **21** were completely purged to the mother liquor.

The optimization of step 3 resulted in the replacement of the hydrogenation catalyst 5% Pd/C type 487 with Pearlman's catalyst at a lower loading (3 vs 7.5 wt %) and an improved direct final product crystallization from MeOH/water. In the initial 30 kg scale-up run of optimized step 3 conditions, a strong exotherm from 25 to 35 °C was observed within the first 10 min.

An unusually high level of C–N hydrogenolysis impurity **24** was observed (10.4 area %) at 1.5 h and this contributed to a low yield (78%). In a second 30 kg run, the reaction temperature was more carefully controlled (22–27 °C) and the charge of Boc-anhydride was slightly increased to 1.03 equiv. In this run, the expected yield of phenol **6** was obtained. The results for these initial 30 kg scale-up runs are summarized below in Table 4.

**Table 4. Summary of the Results for 30 kg Scale Up Runs Producing Phenol 6**

entry	Boc <sub>2</sub> O (equiv)	% yield	assay	purity <sup>a</sup>	residual <b>21</b> <sup>a</sup>	residual Pd (ppm)
1	1.01	78	99.5	99.7	0.20	<10
2	1.03	89	100.1	99.8	0.16	10

<sup>a</sup>Area % by HPLC.

While previous scale ups were performed in headspace reactors, the commercial manufacturer chosen for further scale up uses BCT Loop reactors for improved heat removal and mass transfer efficiencies.<sup>17,18</sup> Because previous studies were performed at pressures of ≤4 bar, additional experiments were evaluated at pressures of 10–40 bar.

At an increased hydrogen pressure of 10–20 bar, a lower level of impurity **20** was observed, while at ≥25 bar, significant amounts of another impurity, **19** (3–5 area %), were observed, indicating a change in the relative rates of reaction of the desired benzyl group cleavage and the C–N ring opening hydrogenolysis. Based on these results, an operating pressure range of 14–16 bar was selected for use.

To eliminate melting of Boc-anhydride prior to its charging, and stability concerns associated with the melted reagent, the use of a stable, 90 wt % solution in THF was adopted.

After reaction completion, the reactor was vented and its contents were heated to 40–50 °C and filtered. A hold time of the reaction slurry at 3–7 °C and a reduction of the water content improved the impurity profile of the crystallized product by keeping impurity **20** in the solution, promoting efficient purging. In the plant, step 3 was run at a 320 kg scale twice daily and reaction solutions were combined for isolation of phenol **6** as a single batch. Table 5 below summarizes the results for a completed registration stability campaign. The step 3 PMI was also reduced from 20 to 9.

**Alkylation and Amidation.** Step 4 in the pilot scale process converted phenol **6** to benzyl ether **8** using 2-fluorobenzyl bromide (**7**) in the presence of K<sub>2</sub>CO<sub>3</sub> in refluxing acetone.<sup>3</sup> The reaction time for this step typically exceeded 50 h. The desired product was crystallized after workup and repetitive codistillations from heptane, which resulted in high solvent usage. In the three chemical transformations for steps 4, 5, and 6, the alkylation, Boc-deprotection, and amidation sequence of reactions start under basic alkylation conditions followed by acidic Boc deprotection and then back to basic amidation conditions. If the two basic reactions were sequential using the same solvent and base, the PMI and efficiency of the

manufacturing operations could be greatly improved using a telescoping approach (Scheme 5).<sup>19</sup>

In the pilot scale process, K<sub>2</sub>CO<sub>3</sub> was used as the base for the alkylation. Therefore, the possibility of using K<sub>2</sub>CO<sub>3</sub> as the base for the step 4 alkylation and a subsequent amidation was explored. This idea was tested and proven to be feasible. To compound **6** and K<sub>2</sub>CO<sub>3</sub> in ACN (5 V) was added 1.05 equiv of bromide **7**. The heterogeneous mixture was heated at 80 °C until compound **6** was ≤2 area % (typically 16 h to 2 d). The batch was cooled to 45 °C and filtered, washed with ACN (2 V), and the filtrate was carried to the amidation step. To the filtered batch, 2.0 equiv of K<sub>2</sub>CO<sub>3</sub> and formamide (2 V; 20 equiv) were added and the mixture was heated to 80 °C until compound **8** was ≤2 area % (typically 16–30 h). To the batch was added water (11 V) at 75–80 °C, followed by cooling to room temperature over 8 h, filtration, washing with water, and drying at 55 °C. To shorten the reaction time, the reaction temperatures for both the alkylation and amidation were raised to 90 °C. This process was scaled to 110 kg (6 batches). The average impurity levels observed (Figure 6) for **8** (intermediate), **27**, and **28** were 1.6, 2.1, and 2.2 area %, respectively, before isolation. After isolation, **26** was obtained in ~90% molar yield and ~96 area % purity; observed levels for **8**, **27**, and **28** were 0.27, 1.2, and <0.05 area %, respectively.

The drawbacks of this alternative process are: (1) two separate charges of potassium carbonate (1.5 equiv for the alkylation and 2.0 equiv for the amidation) and a filtration between reactions were needed; (2) because of the heterogeneity of the reaction mixture, this one-pot process did not scale up consistently in terms of the reaction time for both the alkylation (6–17 h) and the amidation (12–20 h).

In the interest of using a soluble common base for sequential alkylation and amidation steps, it was found that commercially available 25% NaOMe in MeOH was a convenient and inexpensive reagent. An alkylation condition was developed using 1.06 equiv NaOMe/1.10 equiv **7** in dimethylformamide (DMF, 3 V) at 25 °C that reached completion in 1–2 h (*vs* >16 h at 80 °C for the K<sub>2</sub>CO<sub>3</sub> process). ACN was replaced with DMF as this enhanced both reaction kinetics and volumetric efficiency. Following the alkylation step, the telescoped amidation reaction was initiated by adding to the alkylation mixture, 24 equiv of formamide and 1.8 equiv of NaOMe/MeOH at 25 °C.<sup>20</sup> Formamide was added prior to the addition of NaOMe/MeOH to avoid epimerization. The reaction went to completion (<1.0 area % of **8**) in 4 h at 25 °C and similar to the pilot scale process, excess bromide **7** from the alkylation was consumed by N-alkylation of formamide. It was found that there was a clear influence of the equivalents of formamide on the level of all three major impurities, that is, **8**, **27**, and **28** (Figure 7). The level of acid impurity **28** was 2.3 area % with 16 equiv of formamide versus 1.4 area % using 24 equiv. There was a more pronounced effect of the equivalents of formamide on the amount of epimerization impurity **27** (Figure 7). As shown, when 24 equiv of formamide was used, there was significantly less epimerization, likely attributed to a lower basicity.

**Table 5. Summary of the Scale-Up Results for Step 3**

phenol <b>6</b> /batch	% yield	purity <sup>a</sup>	assay	impurities <sup>a</sup>	residual Pd
575–606 kg	86–92%	≥99.8	≥99.6 wt %	≤0.19% <b>20</b> ≤0.08% <b>21</b>	<5 ppm

<sup>a</sup>Area % by HPLC.

## Scheme 5. Alternative Reaction Sequence to 1 Free Base via Boc-Protected Amide 26

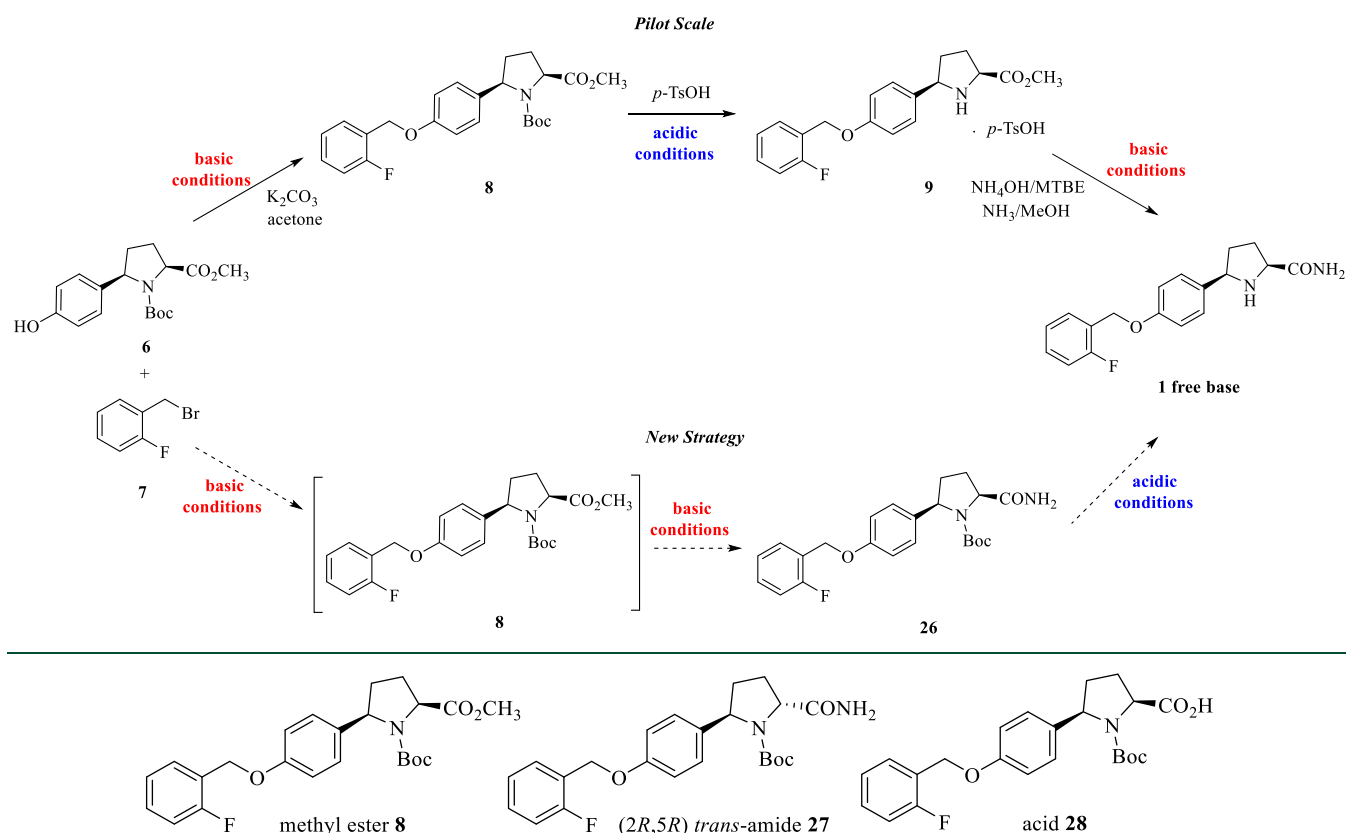


Figure 6. Major impurities observed in telescoped alkylation and ester amidation.

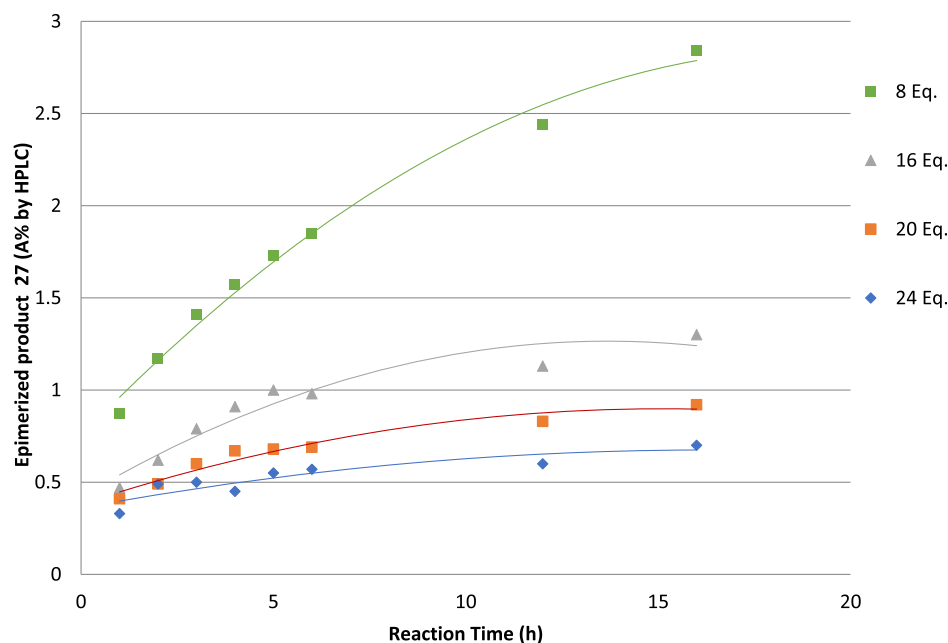


Figure 7. Dependence of the formation of epimerization impurity 27 on reaction time with varying amounts of formamide.

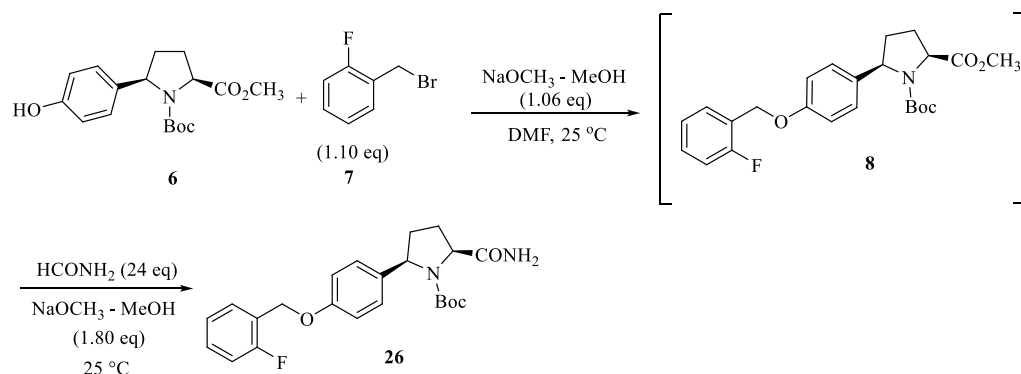
Additionally, when 8 equiv of formamide was used, unreacted **8** did not decrease below 2.7 area % after 17 h. However, when 24 equiv of formamide was used, **8** dropped to <0.7 area % in 3 h.

In summary, compared to the pilot process, the NaOMe one-pot process (Scheme 6) greatly improved the yield of **26** from 90 to 96% and the assay from 96.4 to >99.8%. In terms of

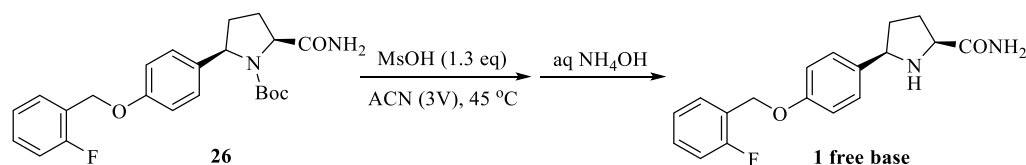
production efficiency, the optimized process resulted in a >50% reduction in the production time and a 2-fold decrease in the volume.

**Deprotection.** The pilot process used *p*-TsOH/MeOH to cleave the Boc group of **8** to provide **9** as its *p*-TsOH salt (Scheme 1). Although the yield and purity of salt **9** was high, the

## Scheme 6. Telescoped Alkylation–Amidation One-Pot Process



## Scheme 7. Deprotection of 26 Using MsOH



process required six extractions (using  $\text{NH}_4\text{OH}$ ,  $\text{Na}_2\text{CO}_3$ , and brine) to remove *p*-TsOH from the product stream, followed by two distillations to replace MTBE with MeOH. In addition, these conditions required development of an analytical method for quantification of residual methyl *p*-toluenesulfonate, a potential mutagenic impurity, in **9**. To replace *p*-TsOH, HCl was considered a favorable choice for the potential benefits of easy removal, low cost, and HCl salt formation at the same time. In one scaled up batch (160 kg **26**), HCl/2-PrOH was used to cleave the Boc group and form HCl salt **1** in 98% yield. In terms of quality, this process did not purge process impurities and gave **1** with nonoptimal physical properties. A recrystallization to purge impurities and control physical properties was performed, but the preference was to control impurities during free base formation and physical properties during the final salt formation. Therefore, this one-pot process condition was not further pursued.

After optimization for both yield and purity, 1.3 equiv of MsOH in ACN (3 V) at 35–45 °C was selected for Boc cleavage to **1** (Scheme 7). Precipitation of **9** as its MsOH salt was observed during the reaction; however, to streamline the process, the MsOH salt was neutralized, in situ, at 50 °C by charging 1.0 N  $\text{NH}_4\text{OH}$  solution (5 V). As the reaction generated 1 equiv each of  $\text{CO}_2$  and isobutylene, an off-gassing safety study was conducted prior to scale up. To control the off-gassing for large-scale production, MsOH was charged slowly over 30 min at 25 °C and the reaction was heated up stagewise to 45 °C. Nucleation occurred toward the end of the  $\text{NH}_4\text{OH}$  addition, after which the mixture was then cooled to 0 °C, filtered, washed with water, and dried to give vixotrigine-free base in 96% molar yield with >99.8 area % purity. These conditions were applied to 700 kg scale batches.

**Final Salt Formation and Particle Engineering.** The pilot process salt formation step (Scheme 1) produced a metastable ethanol solvate of the HCl salt **1**. Although transformation into the desired anhydrous form was observed after drying of the solid, the temperature-driven desolvation process was time consuming and led to shattering of the crystals producing small particles and a wide PSD. These fines did not flow well during the tableting process. To address the poor flow

properties, preblending and roller compaction were required to achieve a blend uniformity suitable for the tableting process. Improvement of the drug substance bulk solid properties would allow for a simpler direct compression (DC) process that would eliminate the need for roller compaction.

It was evident that a desolvation process needed to be avoided to achieve a larger particle size, so 2-PrOH was examined as a replacement for ethanol. The salt formation carried out in 2-PrOH produced the anhydrous HCl salt **1** that did not proceed through a solvate, however, the PSD was still too small to meet formulation needs. Interestingly, it was discovered that replacing gaseous HCl with 6 N aqueous HCl in 2-PrOH produced substantially larger particles as shown in the micrographs in Figure 8.

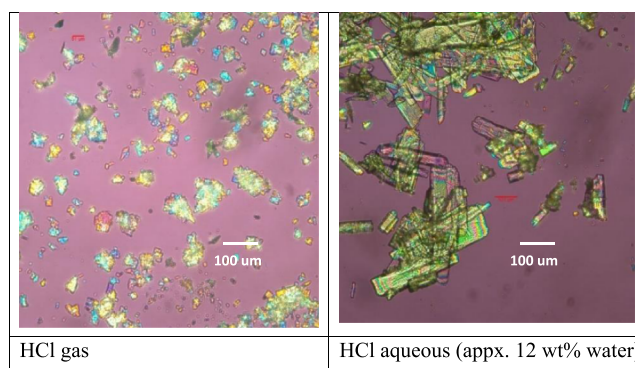


**Figure 8.** PLM images showing differences of **1** produced by HCl gas in 2-PrOH and by aqueous HCl in 2-PrOH (approximately 12% water).

Drug substance particles within a target  $d_{50}$  range of 80–110  $\mu\text{m}$  flowed better and could eliminate the need for roller compaction during drug product manufacturing. Because of low drug substance solubility in 2-PrOH at ambient temperature, the salt formation was performed by direct precipitation of the HCl salt at a higher temperature after dissolving the free base of **1**. The desired particle size in the precipitation process was achieved by controlling the agitation and aqueous acid (1.0

equiv) addition rates. The results from plant campaigns and a comparison with development study lots are summarized in Table 6.

**Table 6. Precipitation Process Scale Up Comparison<sup>a</sup>**

	1 L reactor	500 L reactor	1560 L reactor
batch size (kg)	0.1	45	60
ratio of impeller to tank diameter	0.60	0.56	0.64
aq HCl addition time (min)	2–60 <sup>b</sup>	13.5	30
max agitation speed (rpm)	1000	100	90
max power supplied by the agitation per unit mass slurry (W/kg)	8	0.51	1.47
agitation (rpm)	350–800 <sup>b</sup>	100	90
product PSD ( $\mu\text{m}$ ) <sup>c</sup>			
$d_{10}$	13–19	22	11, 13 <sup>d</sup>
$d_{50}$	60–92	108	86, 96 <sup>d</sup>
$d_{90}$	165–215	252	239, 257 <sup>d</sup>

<sup>a</sup>HCl salt formation was performed by adding 1 equiv of 6 N aq HCl to a free base solution in 6 volumes of 2-PrOH at 65 °C, cooling to 0–5 °C, and filtering and washing the filter cake with 1.5 volumes of 2-PrOH. <sup>b</sup>Range used in development studies. <sup>c</sup>Listed values are volume-based percentiles. <sup>d</sup>Batch 1 and batch 2.

The aq HCl/2-PrOH process did indeed give larger particles; however, the powder blend resulting from the new drug substance was prone to powder consolidation and poor flow when held for ordinary staging periods prior to compression and, therefore, required immediate compression after blending. Further examination of the powder suggested that the increased cohesiveness of the active pharmaceutical ingredient might be because of the presence of large amounts of fines (Figure 10B).

Despite the ability of the alternate precipitation method to produce larger particles, fines were still present, the proportion of which varied from batch to batch. Consistency in PSD and the proportion of fines within the bulk solid were challenging to reproduce in larger vessels with varying impeller and reactor geometries. In order to address the lack of consistency in the particle size, a wet-milling process with temperature cycling was developed in which the product slurry was recirculated through a high-shear mixer, consisting of rotor and stator screens with interchangeable configurations, as depicted in Figure 9. The completion of milling was controlled by in-line particle monitoring (focused beam reflectance measurement), the number of volume turnovers, or a combination of both.

In practice, the salt formation would produce large crystals, wet-milling would follow by circulation of the slurry through a high shear mixer, and then thermal cycling of the wet milled slurry to remove fines prior to the final product isolation. Conditions for each of these stages were selected for development studies, which evaluated the isolated material's bulk and flow properties and tableting feasibility (Figure 10).

The selected final drug substance conditions were demonstrated successfully in large-scale campaigns and produced batches ranging from 120 to 584 kg that met target PSD values (Table 7) for drug product formulation and other key bulk solid-state attributes. This allowed implementation of a DC tableting process for drug product formulation.

Scheme 8 depicts the late-stage process developed to support the production of vixotrigine (1) on a manufacturing scale.

**Summary of Process Improvements to Enable Manufacturing of Vixotrigine at a Late-Stage Scale.**

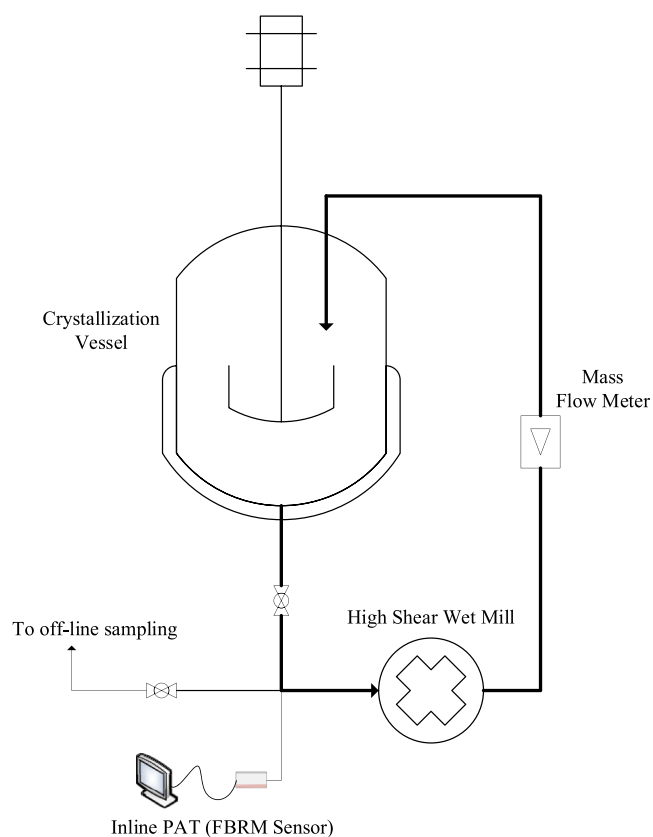


**Figure 9.** Wet mill configuration.

The work described above resulted in a significant improvement in the scalability and robustness of the process and provided a drug substance with preferable solid-state attributes necessary for a DC tableting process. The improvements made for each step of the process are as follows:

- the Grignard reaction stoichiometry was optimized, reducing the charge of aryl bromide **2a** by 17%. Enhanced air-free conditions ensured impurity control while switching from a direct quench to a reverse quench of the reaction mixture, using THF/2-PrOH, allowed for the most efficient utilization of reactors. The flow process described was developed to both enhance process safety for the Grignard formation and remove the reliance on cryogenic reactors during the Grignard addition step.
- for the imine formation, the acid and solvent were changed from TFA/toluene to MsOH/ACN, allowing a purge of any residual impurity **14** via filtration. The acid stoichiometry was reduced to one-third of the original charge, simplifying the neutralization once the reaction endpoint was reached. The reaction quench was optimized by the determination of an optimal pH of its endpoint and ability to be held (7.5), conditions that were most resistant to epimerization of C-2 of the pyrrolidine moiety. Aqueous potassium carbonate (10 V) was replaced by ammonium hydroxide (1.5 V) as the base for the neutralization, effecting a significant improvement in volume efficiency (2.5-fold). The number of unit operations was also significantly reduced.
- the hydrogenation catalyst previously used, 5% Pd/C type 487 paste, was replaced with Pearlman's catalyst [20% Pd(OH)<sub>2</sub>/C], based on the latter's higher activity and selectivity for the target reaction—hydrogenolysis of the

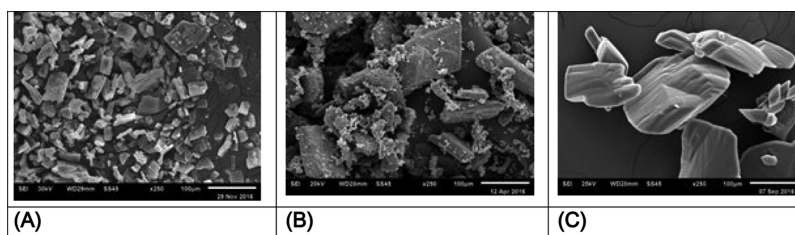


**Figure 10.** Scanning electron microscopy images of **1** produced from three different processing methods. (A) EtOH/HCl gas typical  $d_{50}$ : 15–20  $\mu\text{m}$ . (B) 2-PrOH/aq HCl precipitation typical  $d_{50}$ : 70–110  $\mu\text{m}$ ; note the presence of fines around the larger particles. (C) 2-PrOH/aq HCl crystallization with wet milling and temperature cycling. Typical  $d_{50}$ : 80–125  $\mu\text{m}$ ; note the absence of fines.

**Table 7.** Average PSD Obtained from Large-Scale Manufacturing Campaigns

	batch size (kg)	$d_{10}$ ( $\mu\text{m}$ ) <sup>a</sup>	$d_{50}$ ( $\mu\text{m}$ ) <sup>a</sup>	$d_{90}$ ( $\mu\text{m}$ ) <sup>a</sup>
campaign I	120–174	32	102	217
campaign II	473–584	30	108	256

<sup>a</sup>Listed value is a volume-based percentile.

benzyl group. Catalyst loading was reduced from 7.5 to 3 wt %. A BCT Loop reactor was used to optimize mixing and heat exchange efficiencies. An optimal operating  $\text{H}_2$  pressure of 15 bar was identified, which provided the best hydrogenolysis selectivity (C–O vs C–N). Intermediate **6** was directly isolated from the MeOH reaction solvent after 1.5-fold dilution with water.

- for the alkylation and amidation steps, the sequence of the transformations was changed, so that the two base-mediated reactions, formation of **8** then **26**, were consecutive and could be telescoped to an efficient one-pot process. Problematic removal of *p*-TsOH was solved

by replacement with MsOH for Boc deprotection, which had a dramatic impact on the workup efficiency. The new three reaction sequence (two processing steps) reduced the overall PMI from 106 to 32. In addition, the production time for the combined three steps was reduced 3-fold. Both process steps 4 and 5 gave 96% molar yield with >99.8 area % purity at a 600 kg scale.

- a new HCl salt formation condition was discovered for producing a consistently large PSD material. A wet-milling-temperature cycling operation was added to the process to remove fines and achieve a PSD with desirable flow properties for formulation.

Overall, drug substance batches, on a scale of up to ~600 kg, were able to be reproducibly manufactured, in 54% overall yield, as compared with 43% for pilot scale route 2. Table 8 shows the PMI and yield comparison of the pilot route versus the late-stage route.

**Scheme 8.** Late-Stage Process for Vixotrigine (**1**)

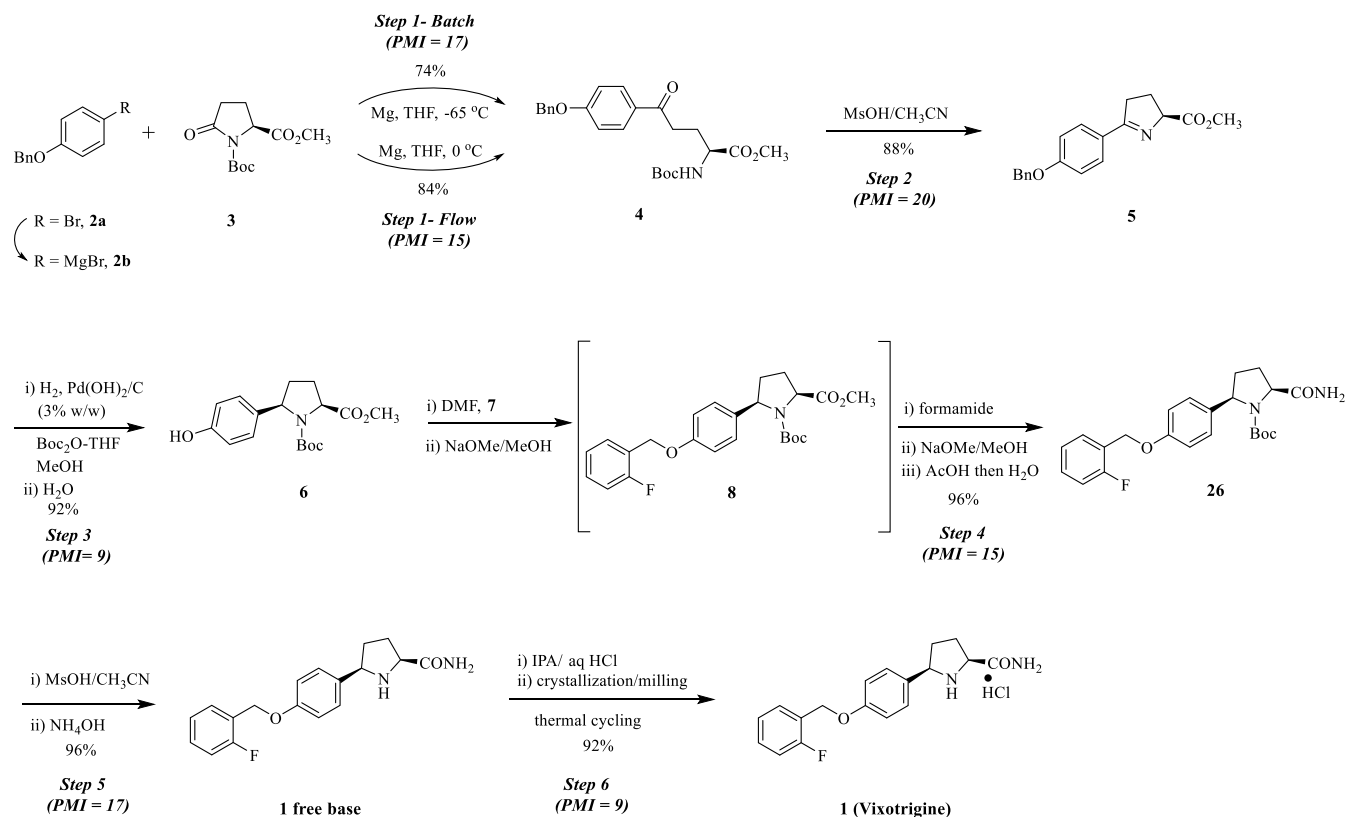


Table 8. PMI and Yield Comparison of the Pilot Route vs the Late-Stage Route

pilot route (cf. Scheme 1)				late-stage route (cf. Scheme 8)			
step	reaction	% yield	PMI	step	reaction	% yield	PMI
1	2b + 3 → 4	78	32	1 (batch)	2b + 3 → 4	74	17
2	4 → 5	90	35	2	4 → 5	88	20
3	5 → 6	87	20	3	5 → 6	92	9
4	6 + 7 → 8	88	39	4	6 + 7 → 26	96	15
5	8 → 9	92	16	5	26 → 1 FB	96	17
6	9 → 1 FB	94	51	6	1 FB → 1 HCl	92	9
7	1 FB → 1 HCl	96	20	1 (flow)	2b + 3 → 4	84	15

## CONCLUSIONS

The pilot scale process, route 2, was optimized to make it amenable to late-stage manufacturing of vixotrigine. The work done simplified operational aspects and improved volume efficiency, the impurity profile, and the overall yield. Step 1 run in a continuous mode was also demonstrated at the kg scale, providing a foundation for further improvement of the process. The overall PMI was reduced by 65% while maintaining drug substance purity at >99.8 area %. Flow properties of the drug substance were improved from the previous process by choosing optimal salt formation and wet-milling conditions. This new process was scaled up to generate 2.5 t of drug substance in a registration campaign with an average yield of 90% for each reaction step.

## EXPERIMENTAL SECTION

**General.** <sup>1</sup>H NMR data were recorded at either 300 or 400 MHz on a Bruker spectrometer. Chemical shifts are expressed as  $\delta$  (ppm) values using the residual signals of the solvents as a reference. LC–mass spectrometry data were generated on an Agilent Q-TOF 6530 spectrometer, operating in ES+ ionization mode, coupled to an Agilent 1290 Series HPLC system. Instrument control and data acquisition were mediated through the MassHunter data acquisition and analysis software.

**Methyl (S)-5-(4-(benzyloxy)phenyl)-2-((tert-butoxycarbonyl)amino)-5-oxopentanoate (4) (Batch Process).** Reactor A was charged with THF (1199 kg) and 1-(benzyloxy)-4-bromobenzene (**2a**; 450 kg). The solids were dissolved by heating to 66 °C, and the solution was degassed by holding at reflux for 10–15 min and cooling to 20–30 °C under an inert atmosphere of nitrogen. Reactor B was charged with Mg (43.6 kg) and THF (399 kg), and DIBAL-H in toluene (1 M; 6.21 kg) was added followed by a toluene (3.19 kg) line rinse, and the mixture was heated to 60–70 °C. To this mixture was added a part of the 1-(benzyloxy)-4-bromobenzene/THF solution from reactor A (80–90 kg) and the resulting mixture stirred for 1 h at 66 °C. After charging additional solution from reactor A (30–40 kg), the initiation of the reaction was checked, and the rest of the solution from reactor A was added to reactor B over 3–4 h while maintaining the mixture under reflux conditions. Reactor A was charged with THF (52 kg), the contents adjusted to 66 °C, and held for 10–15 min, then cooled to 20–30 °C and transferred to reactor B. The contents of reactor B were kept for 50–70 min at 60–70 °C, then cooled to 20–25 °C. Conversion to the Grignard reagent was checked by IPC (HPLC). Reactor C was charged with 1-(tert-butyl)-2-methyl(S)-5-oxopyrrolidine-1,2-dicarboxylate (**3**; 284.9 kg) and THF (760 kg). The solids were dissolved by heating to 66 °C, and the solution was degassed by holding at reflux for 10–15 min. The solution was cooled –60 to –70 °C. To this solution

was added the Grignard solution from reactor B while maintaining a reaction temperature of <–50 °C. Reactor B was rinsed with THF (22 kg) into reactor C and the reaction was aged at <–50 °C for about 1 h. The progress of the reaction was monitored (HPLC). Upon completion, the reaction was quenched by transfer of the reactor C solution into a cold (–20 to 0 °C) solution of 2-PrOH (224 kg) and THF (235 kg) in reactor D while maintaining the temperature at –20 to 0 °C. Reactor C was rinsed with THF (53 kg) into reactor D and the mixture was aged at –20 to 0 °C. Water (712 kg) was added while maintaining an internal temperature of <20 °C. The pH was adjusted to 6.5 by the addition of the aq AcOH solution (50%, ~170 kg) keeping the temperature below 20 °C. The temperature was adjusted to 20–30 °C, the mixture stirred for 20–30 min, and the phases separated (55–65 min). The water phase was discarded and the upper organic layer was treated with NaCl (42 kg) and water (255 kg). The mixture was stirred for 55–65 min and the phases were separated (55–65 min); the water phase was discarded. THF (125 kg) was added to the upper organic phase and the temperature was set to 25 °C. The mixture was then filtered in circulation over a cartridge filter to remove residual magnesium turnings. The filtrate was concentrated under reduced pressure to a residual weight of 1510–1710 kg. The temperature was adjusted to 35–45 °C and *n*-heptane (994 kg) was added and the mixture was stirred for 1–2 h at 35–45 °C. The mixture was then cooled to 15–25 °C over at least 2 h and then to 0–5 °C and stirred for 3–5 h. The solids were isolated by centrifugation and washed with *n*-heptane (291 kg) and then ACN (177 kg) to give 389 kg of the wet product. Based on loss on drying measurements, 375 kg (74%) of the title compound was obtained.<sup>3</sup>

<sup>1</sup>H NMR (400 MHz, CDCl<sub>3</sub>):  $\delta$  1.52 (s, 9H), 2.10 (m, 1H), 2.30 (m, 1H), 2.95–3.15 (m, 2H), 3.76 (s, 3H), 4.40 (m, 1H), 5.15 (s, 2H), 5.18 (br s, 1H), 7.03 (d, *J* = 9 Hz, 2H), 7.30–7.50 (m, 5H), 7.95 (d, *J* = 9 Hz, 2H). MS *m/z*: calcd for C<sub>24</sub>H<sub>30</sub>NO<sub>6</sub> [M + H]<sup>+</sup>, 428.2073; found, 428.2064.

**Methyl (S)-5-(4-(benzyloxy)phenyl)-2-((tert-butoxycarbonyl)amino)-5-oxopentanoate (4) (Flow Process).** The CSTR flow setup consisted of a 1 L stirred tank for reaction, a 1 L settling tank, and a 10 L Schlenk type collection vessel. The stirred tank was equipped with a solid addition device, a reflux condenser, and transfer lines for product solution forward processing. The setup was set to a 500 mL working volume. Step 1: a stirred tank reactor was precharged with THF (70 mL) and magnesium (50.8 g, 5 equiv) and the mixture was stirred at room temperature overnight. The solid addition device was filled with magnesium. The reaction was initiated by adding (4-(benzyloxy)phenyl)magnesium bromide 0.77 M solution in THF (**2b**; 7.7 g, 5.9 mmol). The jacket temperature was increased to 55 °C. A solution of 1-(benzyloxy)-4-bromobenzene (**2a**; 0.85 M in THF) was added to the stirred reaction

vessel. After seven min, the addition of magnesium started at an equimolar rate. The total amount of magnesium for the entire run was 175 g (7.18 mol) and was calculated to keep 5 equiv of magnesium in the stirred tank reactor over the course of the run. When the liquid level in the tank reached operating volume, the product solution was forwarded to the settling tank while maintaining the 500 mL filling level in the CSTR. The approximate residence time of the solution in the jacketed reactor was 62 min. The product was transferred into the settling tank (unstirred), held for the residence time of 1 h, and subsequently transferred to a final collection vessel. The entire process was run for 18 h. Step 2 Grignard addition: the equipment consisted of a tubular pipe reactor, heat exchanger, and a series of centrifugal phase separators. The tubular reactor accommodated mixing of two reagents for the conversion to methyl (S)-5-(4-(benzyloxy)phenyl)-2-((tert-butoxycarbonyl)amino)-5-oxopentanoate (**4**) and quenching of the product solution with an acid solution. The centrifugal phase separators separated the product containing organic phase from the waste aqueous phase. The reagent solutions (methyl *N*-Boc-pyrroglutamate **3**, Grignard **2b**, and sulfuric acid) were transferred continuously at controlled flow rates from their respective storage tank to pass through the tubular pipe reactor, heat exchanger, and finally to the centrifugal extractors. Reaction/quench/workup: the 0.82 M Grignard solution was fed continuously from the storage tank at a molar rate of 1.19 equiv and simultaneously a 0.817 M methyl *N*-Boc-pyrroglutamate **3** solution stream was fed continuously through a heat exchanger to precool it to  $-8^{\circ}\text{C}$ . The tubular reactor for the Grignard addition reaction was attached to a heat exchange unit with chiller fluid set at  $10^{\circ}\text{C}$ . After passing through the reaction zone, 1.0 M sulfuric acid was introduced at a stoichiometric ratio to **3**. The residence time of the solution from reagent introduction to acid quench was 8 s. From sulfuric acid introduction to phase split, the residence time was approximately 80 s. The quenched mixture passed through another heat exchanger to increase the temperature to  $30^{\circ}\text{C}$  for the phase split. This material was directly fed into a centrifugal extractor to remove the aqueous component. The obtained organic layer was subsequently mixed with a solution of brine and sodium bicarbonate in a second centrifugal extractor. The final product-containing organic layer was collected into a glass bottle. The process was run for 3.7 h. Crystallization: the product-containing organic layer was transferred to a 10 L reactor for solvent swap to a low water content THF/heptane solvent system by vacuum distillation. A total of 6867 mL THF (approximately 9.5% v/v) in heptane was added to the reactor and subsequently distilled in approximately two equal portions while maintaining distillation under reduced pressure (approximately 600–700 mbar) at temperatures within  $60$ – $65^{\circ}\text{C}$  to replace the original solvent (water containing THF). The final solution obtained (approximately 11.5 L) was cooled to  $0$ – $5^{\circ}\text{C}$  with a cooling rate of  $0.5^{\circ}\text{C}/\text{min}$  and the resulting slurry was filtered, washed with heptane, and dried under vacuum at  $60^{\circ}\text{C}$  to obtain 1.765 kg (83.6%) of the title compound.

**Methyl (S)-5-(4-(benzyloxy)phenyl)-3,4-dihydro-2H-pyrrole-2-carboxylate (5).** A reactor was charged with methyl (S)-5-(4-(benzyloxy)phenyl)-2-((tert-butoxycarbonyl)amino)-5-oxopentanoate (**4**; 728 kg) and ACN (1715.7 kg) and the slurry temperature was adjusted to  $10$ – $15^{\circ}\text{C}$ . Methanesulfonic acid (474.4 kg) was added in not less than 3 h while maintaining a reaction temperature of  $<26^{\circ}\text{C}$ . The reaction was maintained at  $20$ – $25^{\circ}\text{C}$  for 1 h, then the mixture was cooled  $0$ – $10^{\circ}\text{C}$ . The

conversion was checked by IPC (HPLC). The temperature was adjusted to  $0$ – $5^{\circ}\text{C}$  and the pH was adjusted to  $2$ – $3$  by quick addition of a first part of a solution prepared from water (796 kg) and aq  $\text{NH}_3$  solution (30%, 295.4 kg) keeping the temperature below  $30^{\circ}\text{C}$ . Using the rest of the diluted aq  $\text{NH}_3$  solution, the pH of the mixture was then adjusted more slowly to  $7.5$  ( $7$ – $8$ ) while maintaining a reaction temperature of  $<25^{\circ}\text{C}$ . The phases were separated, and the upper organic layer was heated to  $25$ – $30^{\circ}\text{C}$ . The mixture was filtered over a cartridge filter and the line rinsed with ACN (23.3 kg). A solution of water (909 kg) and 2-PrOH (357 kg) was added at  $20$ – $25^{\circ}\text{C}$ . The solution was cooled to  $15$ – $20^{\circ}\text{C}$  and seeded (3.6 kg). The slurry was cooled to  $0$ – $5^{\circ}\text{C}$  in not less than 2 h and maintained at  $0$ – $5^{\circ}\text{C}$  for at least 30 min. Water (2364 kg) was charged while letting the temperature rise to a maximum of  $20^{\circ}\text{C}$ . The mixture was cooled to  $0$ – $5^{\circ}\text{C}$  and held for 30–40 min, then warmed to  $15$ – $20^{\circ}\text{C}$ , and held for 30–40 min. The slurry was then cooled to  $0$ – $5^{\circ}\text{C}$  in not less than 1 h and maintained for at least 2 h, then filtered. The solids were washed with a mixture of water (1062 kg) and 2-PrOH (279 kg) and dried under reduced pressure at  $50$ – $55^{\circ}\text{C}$  to constant weight to afford 461 kg (88%) of the title compound.<sup>3</sup>

<sup>1</sup>H NMR (400 MHz,  $\text{CDCl}_3$ ):  $\delta$  2.2–2.42 (m, 2H), 2.97 (m, 1H), 3.15 (m, 1H), 3.79 (s, 3H), 4.91 (m, 1H), 5.13 (s, 2H), 7.02 (d,  $J = 9$  Hz, 2H), 7.30–7.50 (m, 5H), 7.86 (d,  $J = 9$  Hz, 2H). MS  $m/z$ : calcd for  $\text{C}_{19}\text{H}_{20}\text{NO}_3$  [ $\text{M} + \text{H}$ ]<sup>+</sup>, 310.1443; found, 310.1438.

**1-(tert-Butyl)2-methyl(2S,5R)-5-(4-hydroxyphenyl)pyrrolidine-1,2-dicarboxylate (6).** A hydrogenation reactor was charged with 20%  $\text{Pd}(\text{OH})_2/\text{C}$  (water wet; 9.6 kg), methyl (S)-5-(4-(benzyloxy)phenyl)-3,4-dihydro-2H-pyrrole-2-carboxylate (**5**; 320 kg activity), MeOH (1142 kg), water (16 kg), and di-*tert*-butyldicarbonate (90% in THF, 250 kg). The reactor was pressurized with nitrogen followed by venting (3 times). The reactor was pressurized with hydrogen followed by venting (3 times). The reactor was pressurized with hydrogen (15 bar). After about 1 h at  $25^{\circ}\text{C}$ , the reactor was vented and repressurized with hydrogen (15 bar). The progress of the reaction was monitored for completion (HPLC). After about 2 h, the reactor was vented and its contents were heated to  $40$ – $50^{\circ}\text{C}$  and filtered, and the filtrate was combined with that from a second identical run. The stream was concentrated in vacuo to about 2800 L at about  $35$ – $40^{\circ}\text{C}$  and at about 240 mbar. The contents of the reactor were cooled to  $20$ – $30^{\circ}\text{C}$  and the formation of a suspension was checked by IPC. The slurry was aged for about 1 h. Water (960 kg) was added over about 1 h. The slurry was cooled to  $3$ – $7^{\circ}\text{C}$  over at least 2 h and aged for about 3 h. The solids were isolated by filtration, washed with 1:4 (v/v) MeOH/water (1226 kg), and dried in vacuo at  $50$ – $55^{\circ}\text{C}$  to a constant weight to afford 605 kg (92%) of the title compound.<sup>3</sup>

<sup>1</sup>H NMR (400 MHz,  $\text{CDCl}_3$ ) (mixture of rotamers):  $\delta$  1.19, 1.43 (2s, 9H), 1.85–2.40 (series of m, 4H), 3.83 (s, 3H), 4.35–5.50 (series of m, 3H), 6.77 (d,  $J = 9$  Hz, 2H), 7.42 (m, 2H). MS  $m/z$ : calcd for  $\text{C}_{17}\text{H}_{23}\text{NNaO}_5$  [ $\text{M} + \text{Na}$ ]<sup>+</sup>, 344.1474; found, 344.1459.

**tert-Butyl (2S,5R)-2-carbamoyl-5-(4-((2-fluorobenzyl)oxy)phenyl)pyrrolidine-1-carboxylate (26).** A reactor was charged with 1-(*tert*-butyl)2-methyl(2S,5R)-5-(4-hydroxyphenyl)pyrrolidine-1,2-dicarboxylate (**6**; 590 kg), anhydrous DMF (1671 kg), and 2-fluorobenzyl bromide [**7**; 382 kg, 1.10 equiv (**caution!** lachrymator!)]. With good stirring, approximately 349 kg (1.06 equiv; assay corrected) of 30% NaOMe solution in

MeOH was added over 60 min while maintaining the temperature between 20 and 30 °C. Following the charge, the line was rinsed forward with MeOH (20 kg) and the batch was maintained between 20 and 30 °C for at least 1 h. The progress of the reaction was monitored for completion (HPLC). Upon completion, formamide (2007 kg) was charged followed by a line rinse with MeOH (20 kg). Approximately 562 kg (1.7 equiv; assay corrected) 30% NaOMe solution in MeOH was added over at least 45 min while maintaining a temperature of between 20 and 30 °C followed by a line rinse with MeOH (20 kg). The contents of the reactor were maintained at about 25 °C with agitation for about 4 h. The progress of the reaction was monitored for completion (HPLC). Upon completion, the batch was transferred to a second reactor and the equipment was rinsed forward with MeOH (172 kg). Glacial acetic acid (217 kg) was added to the batch over at least 10 min while maintaining a temperature of 20–30 °C followed by the addition of water (590 kg). The batch was heated to 60 °C and water (2360 kg) was added over at least 2 h with good agitation. The batch was maintained at 60 °C with agitation for at least 1 h. The batch was cooled to 0–3 °C over at least 3 h and aged for at least 1 h. The solids were isolated by filtration and washed with a mixture of MeOH (280 kg) and water (826 kg) and then with water (1180 kg). The wet cake was dried to constant weight in vacuo at 67 °C to afford 728 kg (95.7%) of the title compound.

<sup>1</sup>H NMR (300 MHz, CDCl<sub>3</sub>): δ 1.13–1.28 (br s, 9H), 1.93–2.09 (m, 2H), 2.25–2.34 (m, 1H), 2.48–2.58 (m, 1H), 4.45–4.53 (m, 1H), 4.60–4.73 (m, 1H), 5.15 (s, 2H), 5.37–5.45 (br s, 1H), 6.93 (d, *J* = 8.7 Hz, 2H), 7.06–7.24 (m, 5H), 7.28–7.37 (m, 1H), 7.48–7.56 (m, 1H). MS *m/z*: calcd for C<sub>23</sub>H<sub>28</sub>FN<sub>2</sub>O<sub>4</sub> [M + H]<sup>+</sup>, 415.2033; found, 415.2028.

(2*S*,5*R*)-5-(4-((2-Fluorobenzyl)oxy)phenyl)pyrrolidine-2-carboxamide (**1 Free Base**). A reactor was charged with *tert*-butyl(2*S*,5*R*)-2-carbamoyl-5-(4-((2-fluorobenzyl)oxy)phenyl)pyrrolidine-1-carboxylate (**26**; 700 kg) and ACN (1287 kg). With good agitation, methanesulfonic acid (208 kg, 1.28 equiv) was added while maintaining a reaction temperature of 20–30 °C followed by ACN (109 kg). The contents of the reactor were warmed to 40–50 °C over at least 30 min and aged for 2–3 h. The progress of the reaction was monitored (HPLC). Upon completion, aq 1.7% NH<sub>3</sub> solution (approximately 693 kg) was added over at least 15 min while maintaining a reaction temperature of 40–50 °C. The reaction temperature was raised to 46–55 °C and aq 1.7% NH<sub>3</sub> solution (approximately 2772 kg) was added over at least 2 h with good stirring and the mixture maintained within this temperature range for 1 h. The slurry was cooled to –3 to 3 °C over at least 3 h and was aged for at least 1 h. The solids were isolated by filtration and washed with a mixture of ACN (111 kg) and water (1259 kg) and then with water (1400 kg). The solids were dried in vacuo at 70 °C for 12 h to afford 507.6 kg (95.6%) of the title compound.<sup>3</sup>

<sup>1</sup>H NMR (400 MHz, CDCl<sub>3</sub>): δ 1.68 (m, 1H), 2.06–2.35 (series of m, 3H), 2.51 (br s, 1H), 3.88 (dd, *J* = 3, 9 Hz, 1H), 4.31 (dd, *J* = 6, 9 Hz, 1H), 5.15 (s, 2H), 5.57 (br s, 1H), 6.99 (d, *J* = 9 Hz, 2H), 7.11 (m, 1H), 7.18 (m, 1H), 7.30–7.40 (m, 3H), 7.53 (m, 1H). MS *m/z*: calcd for C<sub>18</sub>H<sub>20</sub>FN<sub>2</sub>O<sub>2</sub> [M + H]<sup>+</sup>, 315.1509; found, 315.1505.

(2*S*,5*R*)-5-(4-((2-Fluorobenzyl)oxy)phenyl)pyrrolidine-2-carboxamide hydrochloride (**1**). Reactor A was charged with (2*S*,5*R*)-5-(4-((2-fluorobenzyl)oxy)phenyl)pyrrolidine-2-carboxamide (**1 free base**; 473 kg) and 2-PrOH (2339 kg). The contents of the reactor were heated to 70–75 °C, held for 45 min and transferred to reactor B via a filter bag. Reactor A and

the filter line were rinsed with 2-PrOH (74 kg). The contents of reactor B were set to 65–75 °C and purified water (145 kg) was added. The internal temperature was increased to 75 °C and 20% aq hydrochloric acid solution (approximately 274 kg, 1.00 equiv based on the titrated HCl assay) was dosed at an internal temperature of 70–78 °C over 20–40 min. The contents were cooled to 0–15 °C over at least 3 h. The resulting slurry was transferred to reactor C with an installed wet-mill loop and then line rinsed with 2-PrOH (37 kg). The slurry was milled (target 20 passes) while keeping the temperature between 0 and 15 °C. The resulting PSD was controlled by IPC, and the slurry transferred to reactor D at 0–15 °C. Reactor C and the milling equipment were rinsed with 2-PrOH (371 kg) into reactor D. The contents were heated to 60 °C within 3–4 h, held for 10 min at 60 °C then cooled to –2 to 2 °C over 3–4 h. After aging at –2 to 2 °C for 2–3 h, the product suspension was filtered at –2 to 2 °C over a pressure filter. The filter cake was washed under displacement with 2-PrOH (557 kg) via the empty reactor D. The solids were dried in vacuo at 43 °C for 3–4 h and then to constant weight at 68 °C (8 h) to afford 485 kg (91.9%) of the title compound.<sup>3</sup>

<sup>1</sup>H NMR (400 MHz, DMSO-*d*<sub>6</sub>): δ 1.95–2.20 (m, 2H), 2.30 (m, 2H), 3.35 (s, 1H), 4.30 (m, 1H), 4.61 (m, 1H), 5.18 (s, 2H), 7.10 (d, *J* = 9 Hz, 2H), 7.18–7.30 (m, 2H), 7.40 (m, 1H), 7.47 (d, *J* = 9 Hz, 2H), 7.56 (m, 1H), 7.72 (s, 1H), 8.07 (s, 1H), 10.60 (br s, 1H). MS *m/z*: calcd for C<sub>18</sub>H<sub>20</sub>FN<sub>2</sub>O<sub>2</sub> [M + H]<sup>+</sup>, 315.1509; found, 315.1505.

## AUTHOR INFORMATION

### Corresponding Author

Donald G. Walker – Biogen, Product and Technology Development, Cambridge, Massachusetts 02142, United States; [orcid.org/0000-0003-1271-7124](https://orcid.org/0000-0003-1271-7124); Email: [donald.walker@biogen.com](mailto:donald.walker@biogen.com)

### Authors

Robbie Chen – Biogen, Product and Technology Development, Cambridge, Massachusetts 02142, United States  
Vincent Couming – Biogen, Product and Technology Development, Cambridge, Massachusetts 02142, United States  
John Guzowski, Jr. – Biogen, Product and Technology Development, Cambridge, Massachusetts 02142, United States  
Erwin Irdam – Biogen, Product and Technology Development, Cambridge, Massachusetts 02142, United States  
William F. Kiesman – Biogen, Product and Technology Development, Cambridge, Massachusetts 02142, United States  
Daw-Iong Albert Kwok – Biogen, Product and Technology Development, Cambridge, Massachusetts 02142, United States  
Wenli Liang – Biogen, Product and Technology Development, Cambridge, Massachusetts 02142, United States  
Tamera Mack – Biogen, Product and Technology Development, Cambridge, Massachusetts 02142, United States  
Erin M. O'Brien – Biogen, Product and Technology Development, Cambridge, Massachusetts 02142, United States  
Suzanne M. Opalka – Biogen, Product and Technology Development, Cambridge, Massachusetts 02142, United States  
Daniel Patience – Biogen, Product and Technology Development, Cambridge, Massachusetts 02142, United States  
Stefan Sahli – Biogen International, Baar 6340, Switzerland  
Frederick Osei-Yeboah – Biogen, Product and Technology Development, Cambridge, Massachusetts 02142, United States  
Chaozhan Gu – STA Pharmaceutical R&D Company Ltd., A Wuxi AppTec Company, Shanghai 200131, China

**Xin Zhang** – STA Pharmaceutical R&D Company Ltd., A Wuxi AppTec Company, Shanghai 200131, China  
**Markus Stöckli** – Dottikon Exclusive Synthesis AG, Dottikon 5605, Switzerland  
**Thiemo Stucki** – Dottikon Exclusive Synthesis AG, Dottikon 5605, Switzerland  
**Hanspeter Matzinger** – Dottikon Exclusive Synthesis AG, Dottikon 5605, Switzerland  
**Roman Kuhn** – Dottikon Exclusive Synthesis AG, Dottikon 5605, Switzerland  
**Michael Thut** – Dottikon Exclusive Synthesis AG, Dottikon 5605, Switzerland  
**Markus Grohmann** – Dottikon Exclusive Synthesis AG, Dottikon 5605, Switzerland  
**Benjamin Haefner** – Evonik Operations GmbH, Hanau 63457, Germany  
**Joerg Lotz** – Evonik Operations GmbH, Hanau 63457, Germany  
**Michael Nonnenmacher** – Evonik Operations GmbH, Hanau 63457, Germany  
**Paolangelo Cerea** – Olon S.p.A., Milan 20090, Italy

Complete contact information is available at:  
<https://pubs.acs.org/10.1021/acs.oprd.0c00427>

### Author Contributions

This manuscript was written through contributions of all authors. All authors have given approval to the final version of the manuscript. R.C., V.C., J.G., and T.M. were employees of Biogen at the time these studies were conducted. R.C. is currently employed by STA Pharmaceutical R&D Company Ltd., A Wuxi AppTec Company. V.C. is currently employed by Juno Therapeutics, Inc. T.M. is currently employed by Sigilon Therapeutics, Inc. J.G. is currently employed by Translate Bio. E.I., W.F.K., D.-I.A.K., W.L., E.M.O., S.M.O., D.P., S.S., D.G.W., and F.O.-Y. are employees of Biogen and hold stock in Biogen. C.G. and X.Z. are employees of STA Pharmaceutical R&D Company Ltd., A Wuxi AppTec Company that was paid by Biogen to conduct this research. M.S., T.S., H.M., R.K., M.T., and M.G. are employees of Dottikon Exclusive Synthesis that was paid by Biogen to conduct this research. M.N., J.L., and B.H. are employees of Evonik Operations GmbH that was paid by Biogen to conduct this research. P.C. is an employee of Olon S.p.A. that was paid by Biogen to conduct this research.

### Funding

This work was funded by Biogen Inc. and by Convergence Pharmaceuticals Ltd., which has since been acquired by Biogen Inc.

### Notes

The authors declare no competing financial interest.

## ACKNOWLEDGMENTS

The authors wish to sincerely thank Dr. Stuart G. Levy of SGL Chemistry Consulting, LLC for technical assistance in editing this manuscript, a service for which he was financially compensated by Biogen. The authors also wish to thank Dr. Lin Lin of Biogen for the acquisition of supporting analytical data.

## REFERENCES

(1) Obermann, M. Recent advances in understanding/managing trigeminal neuralgia. *F1000Res.* **2019**, *8*, 505.

(2) Zakrzewska, J. M.; Palmer, J.; Ettl, D. A.; Obermann, M.; Giblin, G. M. P.; Morisset, V.; Tate, S.; Gunn, K. Novel design for a phase IIa placebo-controlled, double-blind randomized withdrawal study to evaluate the safety and efficacy of CNV1014802 in patients with trigeminal neuralgia. *Trials* **2013**, *14*, 402.

(3) Giblin, G.; Heseltine, A.; Kiesman, W.; MacPherson, D.; Ramsden, J.; Vadali, R.; Williams, M.; Witty, D. Synthesis of Vixotrigine, a Use-Dependent Sodium Channel Blocker. Part 1: Development of Bulk Supply Routes to Enable Proof of Concept. *Org. Process Res. Dev.* **2020**, DOI: [10.1021/acs.oprd.0c00382](https://doi.org/10.1021/acs.oprd.0c00382).

(4) (a) Process mass intensity (PMI) includes all process materials including water and work-up chemicals relative to the product. (b) Roschangar, F.; Zhou, Y.; Constable, D. J. C.; Colberg, J.; Dickson, D. P.; Dunn, P. J.; Eastgate, M. D.; Gallou, F.; Hayler, J. D.; Koenig, S. G.; Kopach, M. E.; Leahy, D. K.; Mergelsberg, I.; Scholz, U.; Smith, A. G.; Henry, M.; Mulder, J.; Brandenburg, J.; Dehli, J. R.; Fandrick, D. R.; Fandrick, K. R.; Gnad-Badouin, F.; Zerban, G.; Groll, K.; Anastas, P. T.; Sheldon, R. A.; Senanayake, C. H. Inspiring Process Innovation Via an Improved Green Manufacturing Metric: iGAL. *Green Chem.* **2018**, *20*, 2206–2211.

(5) Koch, A.; Dufrois, Q.; Wirgenings, M.; Görls, H.; Kriek, S.; Etienne, M.; Pohnert, G.; Westerhausen, M. Direct Synthesis of Heavy Grignard Reagents: Challenges, Limitations, and Derivatization. *Chem. Eur. J.* **2018**, *24*, 16840–16850.

(6) Tilstam, U.; Weinmann, H. Activation of Mg Metal for Safe Formation of Grignard Reagents on Plant Scale. *Org. Process Res. Dev.* **2002**, *6*, 906–910.

(7) Amaya, T.; Suzuki, R.; Hirao, T. Quinonediimines as Redox-Active Organocatalysts for Oxidative Coupling of Aryl- and Alkenylmagnesium Compounds Under Molecular Oxygen. *Chem. Commun.* **2016**, *52*, 7790–7793.

(8) Baumann, M.; Moody, T. S.; Smyth, M.; Wharry, S. A Perspective on Continuous Flow Chemistry in the Pharmaceutical Industry. *Org. Process Res. Dev.* **2020**, *24*, 1802–1813.

(9) Pastre, J. C.; Browne, D. L.; Ley, S. V. Flow Chemistry Synthesis of Natural Products. *Chem. Soc. Rev.* **2013**, *42*, 8849–8869.

(10) McWilliams, J. C.; Allian, A. D.; Opalka, S. M.; May, S. A.; Journet, M.; Braden, T. M. The Evolving State of Continuous Processing in Pharmaceutical API Manufacturing: A Survey of Pharmaceutical Companies and Contract Manufacturing Organizations. *Org. Process Res. Dev.* **2018**, *22*, 1143–1166.

(11) The process is not fully continuous; **2b** is kept in a storage vessel prior to addition.

(12) Selected publications: (a) Wong, S.-W.; Chang, S. M.; Shields, R.; Bell, W.; McGarvey, B.; Johnson, M. D.; Sun, W.-M.; Braden, T. M.; Kopach, M. E.; Spencer, R. D.; Flanagan, G.; Murray, M. Operation Strategy Development for Grignard Reaction in a Continuous Stirred Tank Reactor. *Org. Process Res. Dev.* **2016**, *20*, 540–550. (b) Hosoya, M.; Nishijima, S.; Kurose, N. Investigation into an Unexpected Impurity: A Practical Approach to Process Development for the Addition of Grignard Reagents to Aldehydes Using Continuous Flow Synthesis. *Org. Process Res. Dev.* **2020**, *24*, 405–414. (c) Hughes, D. L. Applications of Flow Chemistry Drug Development: Highlights of Recent Patent Literature. *Org. Process Res. Dev.* **2018**, *22*, 13–20. (d) Riva, E.; Gagliardi, S.; Martinelli, M.; Passarella, D.; Vigo, D.; Rencurosi, A. Reaction of Grignard Reagents with Carbonyl Compounds under Continuous Flow Conditions. *Tetrahedron* **2010**, *66*, 3242–3247.

(13) For a listing of Johnson Matthey catalysts available for the pharmaceutical market, see: Matthey.com Catalysts For The Pharmaceutical Market|Johnson Matthey. 2020, available online at <https://matthey.com/en/products-and-services/pharmaceutical-and-medical/catalysts?q=>.

(14) Itaya, T.; Morisue, M.; Takeda, M.; Kumazawa, Y. Synthesis of 7-Methyl-3- $\beta$ -D-ribofuranosylwyne, the Putative Structure for the Hypermodified Nucleoside Isolated from Archaeobacterial Transfer Ribonucleic Acids. *Chem. Pharm. Bull.* **1990**, *38*, 2656–2661.

(15) Walker, D. G. Private conversation with Johnson Matthey precious metal catalyst personnel.

(16) Reactions were run in a 1 L Buchi hydrogenator at 5 V. Conversion was comparable at 1.5 and 4 h for the 35 °C, 500 rpm run.

(17) For an animated presentation of a BCT Loop reactor's operation, see: Pratteln-Basel, K. Hydrogenation—Buss Chemtech AG. 2020, available online at [https://www.buss-ct.com/buss\\_loop\\_reactor.html](https://www.buss-ct.com/buss_loop_reactor.html).

(18) For a white paper describing the operating features of a BCT Loop reactor, see: buss-ct.com 2020, available online at [https://www.buss-ct.com/up/files/PDFs\\_RT/Brochure\\_RT\\_Advanced\\_Loop\\_Reactor\\_operating\\_principle.pdf](https://www.buss-ct.com/up/files/PDFs_RT/Brochure_RT_Advanced_Loop_Reactor_operating_principle.pdf).

(19) Gupton, B. F.; McQuade, D. T. A Holistic Approach to Streamlining Pharmaceutical Processes: A Conversation. *Org. Process Res. Dev.* **2019**, *23*, 711–715.

(20) (a) Ramirez, A.; Mudryk, B.; Rossano, L.; Tummala, S. A Mechanistic Study on the Amidation of Esters Mediated by Sodium Formamide. *J. Org. Chem.* **2012**, *77*, 775–779. (b) Wagner, J.; von Matt, P.; Sedrani, R.; Albert, R.; Cooke, N.; Ehrhardt, C.; Geiser, M.; Rummel, G.; Stark, W.; Strauss, A.; Cowan-Jacob, S. W.; Beerli, C.; Weckbecker, G.; Evenou, J.-P.; Zenke, G.; Cottens, S. Discovery of 3-(1*H*-Indol-3-yl)-4-[2-(4-methylpiperazin-1-yl)quinazolin-4-yl]-pyrrole-2,5-dione (AEB071), a Potent and Selective Inhibitor of Protein Kinase C Isoforms. *J. Med. Chem.* **2009**, *52*, 6193–6196.